[CANCER RESEARCH 63, 7883–7890, November 15, 2003]

Soluble Receptor Activator of Nuclear Factor κB Fc Diminishes Prostate Cancer Progression in Bone

Jian Zhang,[1] Jinlu Dai,[2] Zhi Yao,[4] Yi Lu,[4] William Dougall,[5] and Evan T. Keller[1,2,3]

[1]Department of Pathology and [2]Unit for Laboratory Animal Medicine, School of Medicine, and [3]Connective Tissue Oncology Program, Comprehensive Cancer Center, University of Michigan, Ann Arbor, Michigan; [4]Department of Immunology, Tianjin Medical University, Tianjin, China; and [5]Department of Cancer Biology, Amgen, Seattle, Washington

ABSTRACT

Prostate cancer (CaP) develops metastatic bone lesions that consist of a mixture of osteosclerosis and osteolysis. We have previously demonstrated that targeting receptor activator of nuclear factor κB ligand (RANKL) with osteoprotegerin (OPG) prevents the osteolytic activity of CaP and its ability to establish tumor in bone. However, OPG can block tumor necrosis factor-related apoptosis-inducing ligand (TRAIL)-mediated apoptosis, suggesting that the clinical use of OPG may prevent apoptosis of tumors mediated by TRAIL. Thus, methods to block RANKL activity, other than OPG, may be important. Accordingly, we evaluated the ability of soluble murine RANK-Fc (sRANK-Fc) to prevent progression of established CaP in a severe combined immunodeficient mouse implanted with fetal human bone. We first confirmed that sRANK did not block TRAIL-mediated apoptosis of LuCaP cells *in vitro* and that it did block LuCaP-conditioned media-induced osteoclastogenesis *in vitro*. Then, LuCaP 35 CaP cells were injected into the marrow space of the bone implanted in the severe combined immunodeficient mice implanted with fetal human bone and allowed to develop into tumors for 6 weeks. Either vehicle or sRANK-Fc was then administered for 6 weeks. sRANK-Fc diminished tumor-induced osteoblastic lesions as demonstrated by radiograph, bone mineral density measurement, and bone histomorphometry. sRANK-Fc also reduced systemic bone remodeling markers, including serum osteocalcin and bone-specific alkaline phosphatase and urine N-telopeptide of collagen. Finally, sRANK-Fc decreased serum prostate-specific antigen levels and tumor volume in the bone, which indicates decreased tumor burden. In contrast, sRANK-Fc had no effect on s.c. implanted LuCaP cells. We conclude that sRANK-Fc is an effective inhibitor of RANKL that diminishes progression of CaP growth in bone through inhibition of bone remodeling.

INTRODUCTION

The skeleton is the most common site of CaP[6] metastasis, with up to 84% of patients demonstrating skeletal metastases (1). Although characterized radiographically as primarily osteoblastic, it is recognized that CaP skeletal metastases have an extensive bone resorptive component (2, 3). The tumor-induced bone resorption is primarily caused by osteoclasts (4), which accounts for the ability of antiosteoclastogenic agents, such as bisphosphonates that induce osteoclast apoptosis, to diminish tumor-induced osteolysis, decrease pain, and improve mobility in CaP skeletal metastasis patients (5).

Osteoclastogenesis is regulated by a cytokine system consisting of the TNF family member RANKL (also called OPGL, TRANCE, and ODF), its receptor RANK (also called ODAR), and its decoy receptor OPG (also called OCIF and TR1; reviewed in Ref. 6). RANKL, a transmembrane molecule located on bone marrow stromal cells and osteoblasts, binds to RANK, which is located on the surface of osteoclast precursors. This ligand-receptor interaction activates NFκB, which stimulates differentiation of osteoclast precursors to osteoclasts. OPG, also produced by osteoblasts/stromal cells, binds to RANKL, sequestering it from binding to RANK, which results in inhibition of osteoclastogenesis.

We have previously shown that RANKL mediates CaP-induced osteoclastogenesis (7). Furthermore, administration of OPG prevented the establishment of CaP tumor injected into murine bone. These results suggest that blocking RANKL may prevent progression of CaP in bone. However, OPG has been demonstrated to bind the TNF receptor TRAIL and block TRAIL-mediated apoptosis in cancer cells (8, 9). Clinical evidence for the importance of TRAIL-mediated apoptosis is suggested by the observation that TRAIL receptor expression is associated with apoptosis of hepatoma cells (10). Furthermore, TRAIL is considered to be a promising anticancer agent (11, 12). Taken together, these observations suggest that therapeutic use of OPG in clinical cancer may not be prudent because of its potential to protect tumor cells from apoptosis. Thus, development of alternative methods to block RANKL that do not interact with TRAIL may provide useful therapies to prevent CaP progression in bone.

Recently, the use of a sRANK-Fc, which blocks RANKL, was demonstrated to inhibit both lung carcinoma and multiple myeloma-induced bone resorption (13, 14). sRANK-Fc is a chimeric protein formed by fusing the four CRDs of RANK with the Fc portion of human IgG1 (14). The two disulfide bonds of the Fc portion allow homodimerization of the sRANK-Fc proteins, resulting in a homodimer with eight CRDs, which are believed to be responsible for binding to RANKL. The sRANK differs from OPG, which also binds to RANKL, because in addition to containing four CRDs, OPG also has two death domains and a heparin-binding domain (14). These differences in structure between OPG and sRANK-Fc result in different functions between these two molecules including the inability of sRANK-Fc to bind TRAIL. The inability to block TRAIL-mediated apoptosis, yet bind RANKL, suggests that sRANK-Fc may be a useful molecule to prevent progression of CaP in bone. Accordingly, in the current study, we investigated the ability of sRANK-Fc to block the progression of CaP in human bone implanted in a mouse.

MATERIALS AND METHODS

Animals. Male SCID mice (Charles River, Wilmington, MA), 6 weeks of age, were housed under pathogen-free conditions in accordance with the NIH guidelines using an animal protocol approved by the University of Michigan Animal Care and Use Committee.

sRANK-Fc. The sRANK-Fc used in these studies was provided by Amgen Inc. (Seattle, WA) and contains the murine extracellular domain of RANK (through Pro213) fused to human IgG1 Fc. The RANK-Fc protein was produced in Chinese hamster ovary cells as described previously (13, 15).

Preparation of Single-Cell Suspension. LuCaP 35, kindly provided by Dr. Robert Vessella (University of Washington, Seattle, WA), is an androgen-

Received 6/5/03; revised 8/8/03; accepted 9/3/03.

Grant support: Grants from the Army Medical Research and Materiel Command Prostate Cancer Research Program (DAMD17-03-1-0092), National Cancer Institute Specialized Programs of Research Excellence (1 P50 CA69568), University of Michigan Cancer Center Support (5 P30 CA46592), and University of Michigan Program of Comparative Integrative Genomics.

The costs of publication of this article were defrayed in part by the payment of page charges. This article must therefore be hereby marked *advertisement* in accordance with 18 U.S.C. Section 1734 solely to indicate this fact.

Requests for reprints: Evan T. Keller, Room 5304 Cancer Center and Geriatrics Center Building, Box 0940, 1500 East Medical Center Drive, Ann Arbor, MI 48109-0940. Phone: (734) 615-0280; Fax: (734) 936-9220; E-mail: etkeller@umich.edu.

[6] The abbreviations used are: CaP, prostate cancer; TNF, tumor necrosis factor; NF-κB, nuclear factor κB; RANKL, receptor activator of NF-κB ligand; BV:TV, trabecular volume:total bone volume; OPG, osteoprotegerin; TRAIL, tumor necrosis factor-related apoptosis-inducing ligand; CRD, cysteine-rich domain; SCID, severe combined immunodeficient; PSA, prostate-specific antigen; TRAP, tartrate-resistant acid phosphatase; DEXA, dual-energy X-ray absorptiometry; BMD, bone mineral density; BAP, bone-specific alkaline phosphatase; OC, osteocalcin; FBS, fetal bovine serum; CM, conditioned media; NTx, N-telopeptide.

sensitive, PSA-producing human CaP xenograph derived from the lymph nodes of a patient that had failed androgen-deprivation therapy (16, 17). Single-cell suspensions of LuCaP 35 were prepared by resecting the s.c. xenografts and cutting them into small pieces in HBSS with 1% FBS. The small pieces were then rubbed gently between frosted glass slides to obtain single-cell suspensions in HBSS containing 1% FBS. RBCs were lysed with ammonium chloride solution (StemCell Technologies Inc., Vancouver, British Columbia, Canada) and centrifuged at 300 × *g* for 10 min in HBSS with 1% FBS, and the cell pellet was resuspended in RPMI 1640 with 10% FBS. Cell viability was determined by trypan blue counting, and only preparations with >90% viability were used for *in vivo* injection.

Obtaining CM. CM were obtained from cells as described previously (7). Briefly, 5×10^6 cells were plated in 10-cm tissue culture dishes for 12 h in RPMI 1640 with 10% FBS. The media were then changed to 10 ml of RPMI plus 0.5% FBS, and supernatants were collected 24 h later. To normalize for differences in cell density because of proliferation during the culture period, cells from each plate were collected and total DNA content/plate was determined (spectrophotometric absorbance, 260 nm). CM were then normalized for DNA content between samples by adding RPMI.

Treatment. Forty SCID mice had half-sections of human fetal bone (cut in half longitudinally) implanted s.c. as described previously (18). Four weeks later, LuCaP 35 CaP cells (3×10^5 in 50 μl of RPMI 1640 with 10% FBS) were injected into the marrow space of the implanted bone, and tumors were allowed to develop. Six weeks after LuCaP 35 implant, mice were palpated for presence of tumors, which grows out of the open marrow cavity of the bone, and blood was collected and measured for PSA levels (28 of 40 mice had palpable evidence of tumors and were positive for PSA). The mice with tumors were then divided randomly into three groups ($n = 9$/group) to be either immediately sacrificed (basal) or receive either sRANK-Fc (200 μg/mouse) or saline vehicle by i.p. injection three times per week based on a previous study (19). Mice were sacrificed after 6 weeks of sRANK administration. An additional group of mice ($n = 10$) to serve as a control group received bone implants, and 4 weeks after implant (at the same time as the treatment groups received tumor), 50 μl of RPMI with 10% FBS were injected into the marrow cavity, and these mice were sacrificed 6 weeks after injection (in parallel with the basal group). Serum, urine, and bones were collected for evaluation. Before sacrifice, the animals were anesthetized, and magnified flat radiographs were taken with a Faxitron (Faxitron X-Ray Corp., Wheeling, IL).

Histopathology and Bone Histomorphometry. Histopathology was performed as described previously (7). Briefly, bone specimens were fixed in 10% formalin for 24 h, then decalcified using 12% EDTA for 72 h. The specimens were then paraffin embedded, sectioned (5 μM), and stained with H&E to assess histology or stained with TRAP to identify osteoclasts. Four discontinuous random regions of interest were examined within each bone implant to represent the bone fragment. To perform TRAP staining, nonstained sections were deparaffinized and rehydrated, then stained for TRAP (acid phosphatase kit, model 387-A; Sigma Diagnostics, St. Louis, MO) as directed by the manufacturer with minor modification. Briefly, the specimens were fixed for 30 s and then stained with acid phosphatase and tartrate solution for 1 h at 37°C, followed by counterstaining with hematoxylin solution. Osteoclasts were determined as TRAP-positive staining multinuclear (>3 nuclei) cells by light microscopy. Histomorphometric analysis was performed on a BIOQUANT system (R&M Biometrics, Inc., Nashville, TN) as described previously (20). The terminology used was that recommended by the Histomorphometry Nomenclature Committee of the American Society for Bone and Mineral Research (21). Tumor area was determined as the proportion of tumor area in the total nonmineralized portion of the bone.

DEXA Measurement and X-Ray. BMD of the excised bone implants was measured using DEXA on an Eclipse Peripheral Dexa Scanner using pDEXA Sabre software, version 3.9.4, in research mode (Norland Medical Systems, Fort Atkinson, WI). Excised implants were scanned at 2 mm/s with a resolution of 0.1 × 0.1 mm. Three 0.5-cm regions of interest were selected randomly for each fragment to determine BMD. Short-term BMD precision (percentage of coefficient of variation) was ~3% for this technique. Radiographs were taken before the sacrifice of the animals and after the excision of bone implants by using a Faxitron.

PSA Measurement. Total PSA levels in serum were determined using the Accucyte Human PSA assay (Cytimmune Sciences Inc., College Park, MA). The sensitivity of this assay is 0.488 mg/ml.

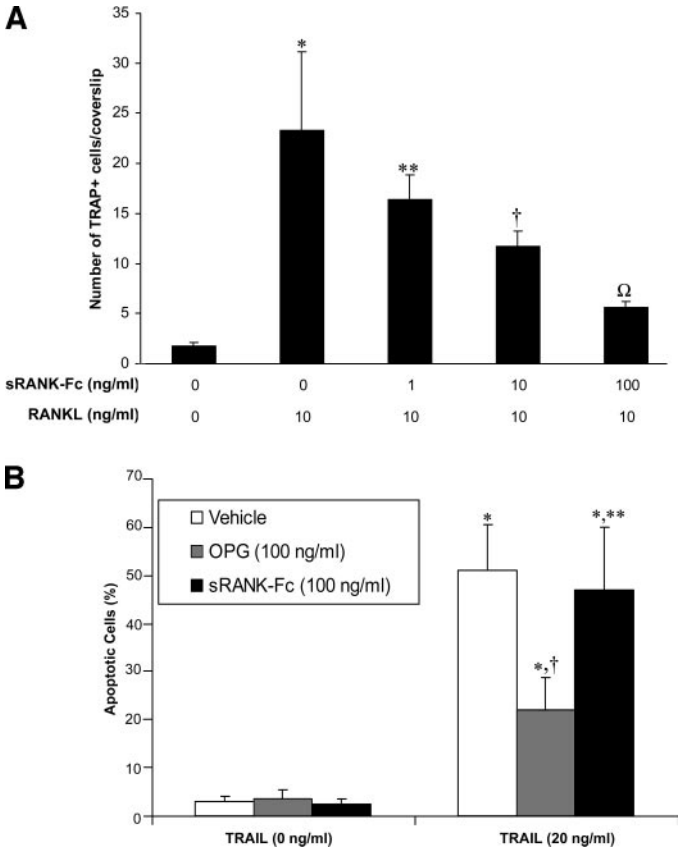

Fig. 1. Effect of sRANK-Fc on RANKL activity and TRAIL-mediated apoptosis *in vitro*. *A*, single-cell suspensions of RAW 264.7 cells were plated in 24-well plates (1×10^5 cells/well) on top of sterile coverslips in RPMI plus 10% FBS. Cells were grown for 12 h, then the media were changed to RPMI plus 0.5% FBS, and recombinant human sRANKL (10 ng/ml) and sRANK-Fc were added as indicated. Osteoclasts were identified as TRAP-positive multinucleated (>3 nuclei) cells, and the number of osteoclasts per coverslip were quantified. Data are reported as the mean ± SD of triplicates from two independent experiments. *, $P < 0.001$ compared with nontreatment culture; **, $P < 0.05$ compared with the RANKL only treatment; †, $P < 0.01$ compared with RANKL only and $P < 0.05$ compared with 1 ng/ml sRANK-Fc treatment; Ω, $P < 0.01$ compared with RANKL only and 1 ng/ml and 10 ng/ml sRANK-Fc treatments (one-way ANOVA and Fisher's protected least significant difference for *post hoc* analysis). *B*, LuCaP cells were plated (1×10^6/well) in 12-well plates in RPMI plus 10% FBS. After 12 h of culture, media were changed to RPMI plus 0.5% FBS, and OPG, sRANK-Fc, or TRAIL was added as indicated. After an additional 24 h of culture, cells were assessed for apoptosis on a fluorescent microscope using Annexin V-FITC staining. Results are reported as the mean ± SD of two experiments. *, $P < 0.01$ compared with no TRAIL for each respective compound; †, $P < 0.01$ compared with TRAIL-treated vehicle group; **, $P < 0.01$ compared with TRAIL-treated OPG group (ANOVA and Fisher's protected least significant difference for *post hoc* analysis).

Serum OC Measurement. Serum human OC was measured by a competitive immunoassay kit (Metra Osteocalcin, Quidel Corporation, Santa Clara, CA). The assay does not cross-react with murine OC. This antibody is conformationally dependent and recognizes only intact (*de novo*) OC and not fragments from resorbed bone tissues. The sensitivity of this assay is 0.45 ng/ml.

Serum BAP Measurement. Serum human BAP was measured by an immunoassay kit (Metra BAP EIA, Quidel Corporation, Santa Clara, CA). This assay does not cross-react with murine BAP. The sensitivity of this assay is 0.7 units/liter.

Urine NTx and Creatinine Measurements. Urine NTx was measured using human-specific ELISA, as recommended by the manufacturer (Osteomark NTx; Ostex Inc.). Results were reported as a ratio of NTx bone collagen equivalents (nanomolar bone collagen equivalents) to urine creatinine (millimole creatinine). Urine creatinine was measured using a creatinine kit (Metra Biosystems, Mountain View, CA) as directed by the manufacturer.

Cell Viability. Single-cell suspension of LuCaP cells were plated at 2×10^6/plate in 60-mm plates in triplicates with RPMI and 10% FBS. After 12 h of culture, media were changed to RPMI plus 0.5% FBS and sRANK-Fc

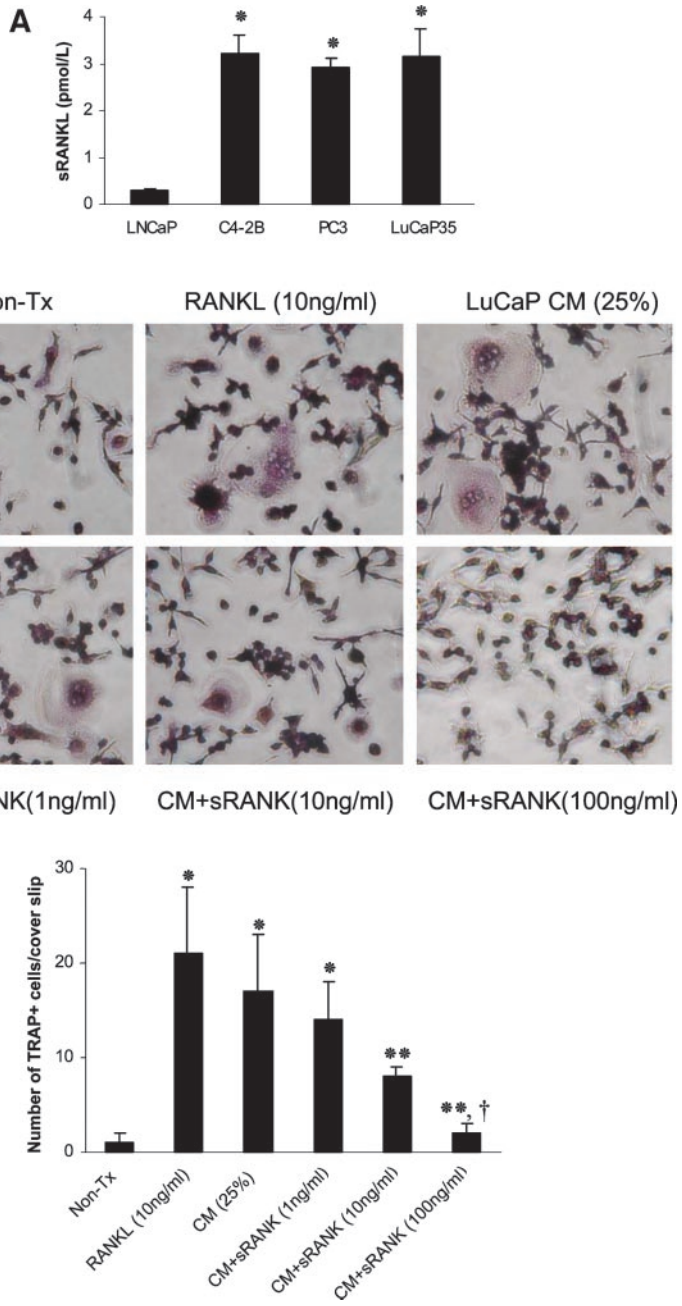

Fig. 2. Effects of sRANK-Fc on CaP-induced osteoclast activity *in vitro*. *A*, LNCaP, C4–2B, PC3, and LuCaP 35 cells were plated (5×10^5 cells) in 12-well plates. After 24 h, CM were collected and subjected high-sensitivity ELISA for sRANKL. Data are reported as the mean ± SD of three experiments. *, $P < 0.05$ compared with LNCaP (one-way ANOVA and Fisher's protected least significant difference for *post hoc* analysis). *B*, representative pictures of cultures stained for TRAP. Single-cell suspensions of RAW 264.7 cells were plated in 24-well plates (1×10^5 cells/well) on top of sterile coverslips in RPMI plus 10% FBS. Cells were grown for 12 h, then the media were changed to RPMI plus 0.5% FBS. Either recombinant human sRANKL (10 ng/ml) or CM harvested (as described in "Materials and Methods") from LuCaP cells was added to a final concentration of 25% (vol/vol) as indicated. Immediately, the indicated concentration of sRANK-Fc was added. Osteoclasts were identified as TRAP-positive multinucleated (>3 nuclei) cells. *C*, number of osteoclasts per coverslip were quantified. Data are reported as the mean ± SD of quadruplicates from two independent experiments. *, $P < 0.001$ compared with nontreatment culture; **, $P < 0.05$ compared with the CM-treated culture and 1 ng/ml treatment; †, $P < 0.01$ compared with 10 ng/ml treatement (one-way ANOVA and Fisher's protected least significant difference for *post hoc* analysis).

was added at different concentrations, and 24 h after an additional 24 h, cells were collected and viability was examined by trypan blue exclusion.

Cell Proliferation. Cell proliferation was measured using the CellTiter 96 AQ Non-radioactive cell proliferation assay (Promega, Madison, WI). Briefly, LuCaP cells in RPMI plus 5% FBS were added to the wells of a 96-well plates at 5000/well in triplicates. After 12 h of culture, the media were changed to RPMI plus 0.5% FBS, and a different concentration of sRANK-Fc was added. Cells were allowed to grow for 24 h, then 20 μl/well of combined MTS/PMS solution were added. After incubation of 1 h at 37°C in a humidified 5% CO_2 atmosphere, the absorbance at 490 nm was recorded by using an ELISA plate reader.

Cell Apoptosis. LuCaP cells were plated at 1×10^6/well in 12-well plates on sterile coverslips in triplicate with RPMI plus 10% FBS. After 12 h of culture, media were changed to RPMI plus 0.5% FBS and immediately a different concentration of recombinant OPG (R&D Systems Inc.), sRANK-Fc, or TRAIL (R&D Systems, Inc.) was added. Subsequently, cells were evaluated for apoptosis on a fluorescent microscope using Annexin V-FITC detection kit (PharMingen, San Diego, CA) following the manufacturer's protocol. Ten random ×50 fields were counted, and the results are reported as percentage of FITC-positive cells.

Statistical Analysis. Statistical analysis was performed using Statview software (Abacus Concepts, Berkley, CA). ANOVA was used for initial analyses, followed by Fisher's protected least significant difference for *post hoc* analyses. Differences with a $P < 0.05$ were determined as statistically significant.

RESULTS

RANKL is a key inducer of osteoclastogenesis. To ensure that sRANK-Fc blocks RANKL-induced osteoclastogenesis *in vitro*, we coincubated osteoclast precursor RAW cells with RANKL in the presence of increasing doses of sRANK-Fc. RANKL-induced osteoclastogenesis and sRANK-Fc inhibited the osteoclastogenesis in a dose-responsive fashion (Fig. 1*A*). OPG has been shown to bind TRAIL (22) and block TRAIL-mediated apoptosis in CaP cells *in*

vitro (9), which suggests that it may be protect cancer cells against TRAIL-mediated apoptosis *in vivo*. Accordingly, other factors to block RANKL that do not block the proapoptotic activity of TRAIL may be useful for cancer therapy. We have determined that sRANK-Fc does not bind TRAIL (data not shown); however, to ensure that it does not block TRAIL-mediated apoptosis, we tested the effect of sRANK-Fc on TRAIL-mediated apoptosis of LuCaP cells. We found that although OPG diminished TRAIL-mediated apoptosis of LuCaP cells, sRANK-Fc had no effect (Fig. 1*B*). These data demonstrate that sRANK-Fc blocks RANKL-induced osteoclastogenesis but does not protect LucCaP cells against TRAIL-mediated apoptosis.

To determine whether LuCaP 35 cells produce sRANKL, we created single-cell suspensions of LuCaP 35 and grew them for 24 h, then collected the culture supernatants to test for sRANKL expression. LuCaP 35 cells secreted sRANKL at levels similar to C4–2B and PC-3 CaP cells, but ~8-fold higher levels than LNCaP CaP cells (Fig. 2*A*). To determine whether sRANK-Fc could inhibit LuCaP-induced osteoclastogenesis, we incubated osteoclast precursor RAW cells with LuCaP CM in the absence and presence of sRANK-Fc. LuCaP CM induced osteoclasts, and sRANK-Fc decreased LuCaP-mediated osteoclastogenesis in a dose-responsive fashion (Fig. 2, *B* and *C*). These data demonstrate that LuCaP35 produces functional sRANKL and that LuCaP-induced osteoclastogenesis can be inhibited by sRANK-Fc.

To evaluate the ability of sRANK-Fc to prevent progression of established CaP in bone, we s.c. implanted human fetal bone into 40 SCID mice. Four weeks later, LuCaP 35 CaP cells were injected into the marrow space of the implanted bone and allowed to develop into tumors. Six weeks after tumor implant, mice were palpated for presence of tumors. We determined that 28 of 40 mice had palpable evidence of tumor growth in the implanted bone (70% tumor take-up rate in the bone at 6 weeks). To confirm that these 28 mice had LuCaP xenograft growth, we measured serum PSA levels. The mouse does not produce PSA, thus this measurement is a specific marker of human CaP tumor in these animals. All 28 mice were positive for PSA (mean ± SD, 13.2 ± 3.1 ng/ml). The mice with PSA-confirmed tumors were then divided randomly into three groups (n = 9/group; one mouse was not used; serum PSA levels were not statistically different among groups) to be either immediately sacrificed (basal) or receive either sRANK-Fc (200 μg/mouse) or saline vehicle by i.p. injection three times per week. Mice were sacrificed after 6 weeks of sRANK administration.

The presence of LuCaP tumors for 6 weeks induced an osteosclerotic radiographic response (Fig. 3*A*, basal *versus* control). After an additional 6 weeks of tumor growth (12 weeks total), the radiographic osteosclerotic appearance increased in the vehicle-treated animals (Fig. 3, vehicle *versus* basal), whereas sRANK-Fc diminished the osteosclerotic appearance (Fig. 3*A*, sRANK-Fc *versus* vehicle), although it was still increased over that of the basal group. To accurately quantify differences in BMD, we used DEXA (Fig. 3, *A* and *B*). The BMD was increased by 15% in the basal group compared with the control group (mice implanted with human fetal bone without tumor). After an additional 6 weeks, the BMD was increased by 12% in the vehicle-treated group compared with the basal group. In contrast, sRANK-Fc limited the increase of BMD to 4% (*i.e.*, ~67% lower increase of BMD then occurred in the vehicle group). These results indicate that LuCaP 35 induces an osteoblastic lesion and that sRANK-Fc inhibits tumor-induced bone formation.

To evaluate the effects of sRANK-Fc at the cellular level of bone, we performed bone histomorphometry on excised implants. The BV:TV, which represents the proportion of total mineralized trabeculae in the total bone in the section, was increased by 19% in the basal group

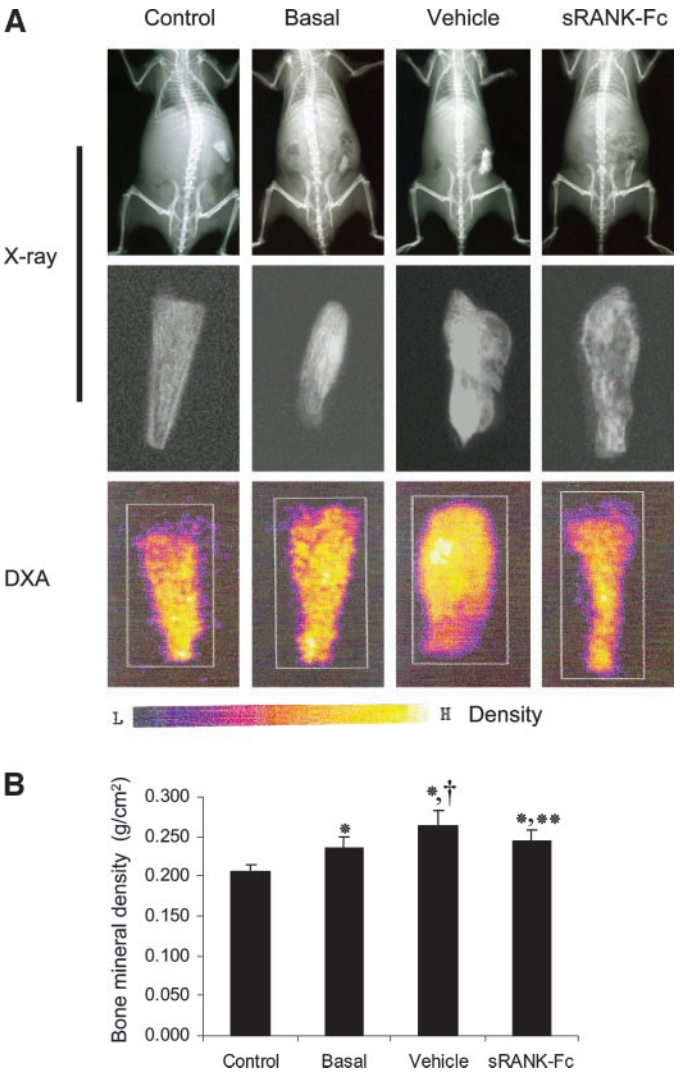

Fig. 3. Radiological examination of LuCaP-induced bone lesions. Implanted human fetal bones in SCID mice were injected with LuCaP 35 single-cell suspension. Six weeks after tumor injection, some mice were sacrificed as the basal group (n = 9). The remaining mice were divided to receive either sRANK-Fc (200 μg/kg) or vehicle (1% BSA in PBS; n = 9/group). Treatments were administered via i.p. injection three times per week for 6 weeks, and the mice were then sacrificed. *A*, radiograph of LuCaP-induced bone lesions determined by X-ray and DEXA showing osteoblastic lesions with stronger density of the tumor implants compared with the control group (without tumor implantation). Measurement of BMD was performed using DEXA. The color scale indicates low (*L*) density through high (*H*) density. *B*, quantification of BMD for the excised implants in different groups. Values are presented as mean ± SD. *, $P < 0.01$ compared with control group; †, $P < 0.05$ compared with basal group; **, $P < 0.05$ compared with vehicle-treated group (one-way ANOVA and Fisher's protected least significant difference for *post hoc* analysis).

compared with the control group (Fig. 4*A*). The BV:TV continued to increase by an additional 11% in the vehicle-treated group compared with the basal group (overall 30% increase in the vehicle group compared with the control group). Administration of sRANK-Fc diminished the increase of BV:TV by 83% (Fig. 4*A*, sRANK-Fc *versus* vehicle). The osteoblast perimeter (*ObS/BS*), which represents the number of osteoblasts per millimeter of trabecular bone, was increased by 132% and 152% in the basal and vehicle-treated groups, respectively, compared with the control group (Fig. 4*B*). Administration of sRANK-Fc did not alter the increase of osteoblast perimeter that occurred in the vehicle-treated group (sRANK-Fc *versus* vehicle). Osteoclast perimeter (*Oc/BS*), which represents the number of osteoclasts per millimeter of trabecular bone, was increased by ~720% in the basal group *versus* control group (Fig. 4*C*), indicating that LuCaP

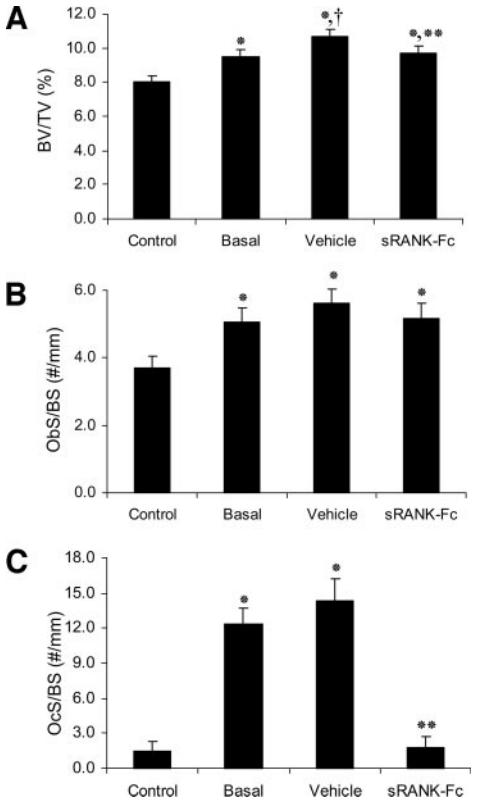

Fig. 4. Effects of sRANK-Fc on bone histomorphometric parameters of LuCaP-induced osteoblastic lesions. Three nonserial sections of each implant were analyzed by using the Bioquant system as described in "Materials and Methods." Five random ×200 magnification fields were evaluated per each section. The values are reported as mean ± SD ($n = 9$ mice/group). Data were analyzed using one-way ANOVA and Fisher's least significant difference for *post hoc* analysis. *A*, the BV:TV was used to represent total mineralized bone in the trabeculae. ∗, $P < 0.05$ compared with control; †, $P < 0.01$ compared with basal; ∗∗, $P < 0.05$ compared with vehicle-treated group. *B*, the osteoblast perimeter (*ObS/BS*) represents the number of osteoblasts per millimeter length of bone interface. ∗, $P < 0.001$ compared with control. *C*, the osteoclast perimeter (*OcS/BS*) represents the number of osteoclasts per millimeter length of tumor-bone interface. ∗, $P < 0.001$ compared with control; ∗∗, $P < 0.001$ compared with vehicle-treated group.

35 induces osteoclastogenesis. However, it was not further increased in the vehicle-treated mice *versus* basal mice. Administration of sRANK-Fc decreased the osteoclast perimeter to levels similar to the control mice. These results indicate that LuCaP 35 induces both an osteoblastic and osteoclastic responses in bone that can both be inhibited by sRANK-Fc.

To determine whether the tumor-induced changes in bone were reflected systemically in the animals, several bone remodeling markers were measured. Serum human OC, BAP, and urinary Ntx, an indicator of bone resorption, were evaluated. These compounds were not detectable in the control mice (data not shown) although they were detectable in the basal group (Fig. 5). Serum human OC and BAP were decreased by ~30% and 25%, respectively, in the sRANK-Fc-treated mice compared with the vehicle-treated mice (Fig. 5, *A* and *B*). Urinary NTx was reduced by 30% in the sRANK-Fc-treated mice compared with the vehicle-treated mice (Fig. 5*C*).

To determine the extent of tumor burden, we quantified serum PSA levels in mice. Serum PSA levels, which were undetectable in control mice (data not shown), were increased by ~157% in the vehicle-treated mice compared with the basal mice (Fig. 6*A*). Administration of sRANK-Fc resulted in only a 50% increase in PSA levels from the levels of basal mice, thus diminishing the increase in that occurred in the vehicle group by ~66% (Fig. 6*A*). Tumor that stained positive for PSA was readily identified in all of the mice in the various tumor-injected groups (Fig. 6*B*). Tumor area/total nonmineralized bone area was increased by 60% in the vehicle-treated group compared with the basal group (represents continued tumor growth; Fig. 6*C*). In the group receiving sRANK-Fc, the tumor area was increased by 32% compared with the basal group but this was ~50% less than the increase observed in the vehicle-treated group (Fig. 6*C*). These results showed that sRANK-Fc diminishes LuCaP 35 tumor progression in bone.

To explore whether the ability of sRANK-Fc to inhibit lesions in the bone was a direct effect on tumor cells, we incubated LuCaP 35 cells with sRANK-Fc, then evaluated proliferation rate and cell viability. sRANK-Fc had no effect on these proliferation rates or viability of the LuCaP cells (data not shown). Additionally, we injected LuCaP cells s.c. into the mice, allowed tumors to develop for 6 weeks, then administered sRANK-Fc in a similar fashion as for the studies performed with bone. Administration of sRANK-Fc had no effect on s.c. LuCaP 35 tumor growth rate (Fig. 7). These data suggest that sRANK-Fc does not have a direct inhibitory effect on LuCaP 35.

DISCUSSION

The results from the present study demonstrate that sRANK-Fc diminishes CaP progression in osseous, but not in nonosseous, tissue. Furthermore, the observation that sRANK-Fc did not diminish s.c. growth of the tumor, in combination with the observation that it had no direct affect on the CaP cells *in vitro*, suggests that the ability of sRANK-Fc to inhibit CaP establishment was not because of a direct

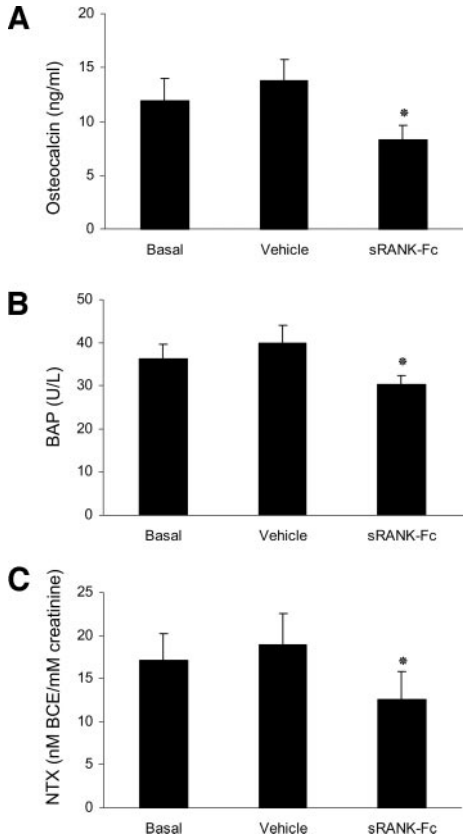

Fig. 5. Effect of sRANK-FC on systemic bone remodeling markers. Serum and urine were collected from basal, sRANK-Fc, and vehicle treatment groups at the time of their euthanasia. Serum OC, serum BAP, urine NTx, and urine creatinine were measured as described in "Materials and Methods." *A*, serum OC levels. *B*, serum BAP levels. *C*, urine NTx levels are reported as bone collagen equivalents (*BCE*) normalized to urine creatinine levels. Data are reported as mean ± SD. Data were analyzed using one-way ANOVA and Fisher's protected least significant difference for *post hoc* analysis. ∗, $P < 0.01$ compared with vehicle-treated group. Measurements were performed in six to nine individual mice per group.

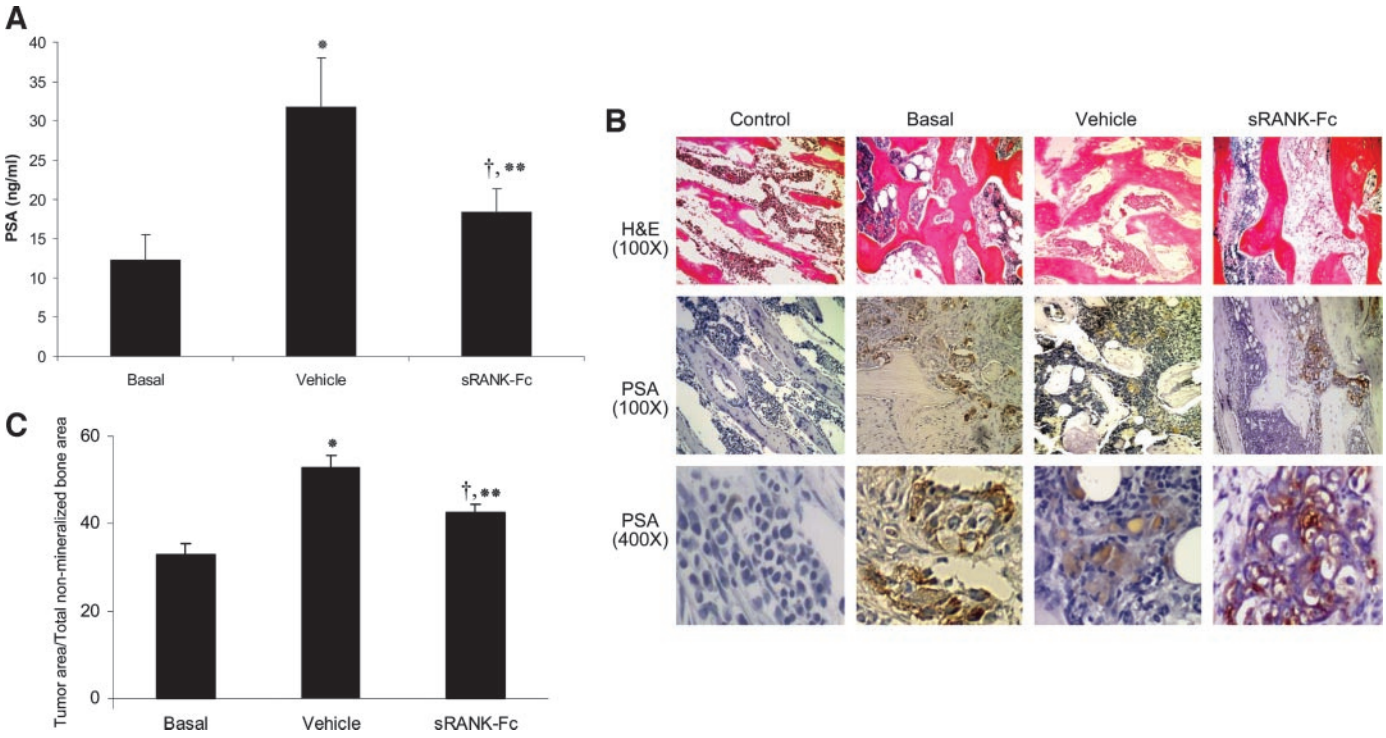

Fig. 6. Effect of sRANK-Fc on LuCaP tumor burden. *A*, serum was collected from basal, sRANK-Fc, and vehicle treatment groups at the time of their euthanasia and subjected to ELISA for PSA. Values are reported as mean ± SD ($n = 9$/group). *, $P < 0.001$ compared with basal group; †, $P < 0.01$ compared with basal; **, $P < 0.01$ compared with vehicle-treated group (one-way ANOVA and Fisher's least significant difference for *post hoc* analysis). *B*, histological examination of LuCaP tumors growing in human fetal bone implanted into SCID mice. Formalin-fixed paraffin-embedded sections were stained with H&E or were deparaffinized, rehydrated, and stained for PSA using immunohistochemistry. *Brown* indicates positive staining of PSA. Representative H&E staining of normal implanted fetal bone without tumor implantation, and implant from mice of basal, vehicle, and sRANK-Fc treatment that paralleled with representative slides of PSA-stained sections were presented. Note in control mice the marrow compartment of human fetal bone implants contain mainly stromal elements and some residual hematopoietic cells, and in tumor implants, the bone marrow contains tumor cells. Specifically, the intramedullary space from the basal and vehicle-treated groups (×100) has a large component of PSA-positive cells compared with the sRANK-Fc-treated groups. Also, note the increased amount of trabeculae (*red*) and corresponding decrease in marrow space in the in the basal and vehicle-treated groups compared with the control or sRANK-Fc-treated groups. *C*, bone tumor burden (total tumor volume as a percentage of noncalcified tissue volume) was determined using bone histomorphometric analysis. Three nonserial sections of each implant were analyzed by using the Bioquant system as described in "Materials and Methods." Five random ×200 magnification fields were evaluated per each section. The values are reported as mean ± SD ($n = 9$ mice/group). *, $P < 0.001$ compared with basal group; †, $P < 0.01$ compared with basal; **, $P < 0.01$ compared with vehicle-treated group (one-way ANOVA and Fisher's protected least significant difference for *post hoc* analysis).

effect on tumor but rather specific to factors in the bone microenvironment. These data suggest that inhibition of RANKL activity diminishes the progression of CaP skeletal metastasis.

The importance of osteoclastic activity in the development of CaP skeletal metastatic lesions has received little attention because of their overall osteoblastic radiographic appearance. Yet, despite the radiographic appearance, it is clear from histological evidence that CaP metastases form a heterogeneous mixture of osteolytic and osteoblastic lesions (2, 3, 23–25). In fact, histomorphometric analysis of metastatic lesions reveals that osteoblastic metastases form on trabecular bone at sites of previous osteoclastic resorption, suggesting that bone resorption is required for subsequent osteoblastic bone formation (2). Results from the current study are consistent with previous studies that demonstrate inhibition of RANKL with OPG diminishes CaP establishment or progression of established tumor in bone (7, 26). Taken together, these results support previous published evidence that tumors that metastasize to bone require osteoclastic activity, which releases tumor-supportive growth factors from bone (27, 28). They further extend these studies, because LuCaP is clearly an osteoblastic tumor, as demonstrated by radiographs, DEXA, and bone histomorphometry. Thus, these data clearly demonstrate that osteoclast activity is necessary for the development of osteoblastic CaP tumors.

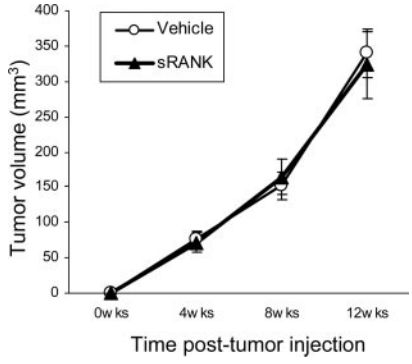

Fig. 7. Effect of sRANK-Fc on s.c. implanted LuCaP tumor growth. LuCaP cells were s.c. injected into SCID mice, and tumors were allowed to develop for 6 weeks, then sRANK-Fc (200 μg/mouse/day) or vehicle (1% BSA in PBS) were administered via i.p. injection three times per week for 6 weeks, and the mice were then sacrificed. The tumor volume was measured every 4 weeks. The values are reported as mean ± SD.

An active role for osteoclast activity in prostate tumor bone metastasis development is also reflected in clinical data that demonstrate systemic markers of bone resorption are increased in men with CaP skeletal metastases (29, 30) and that bisphosphonates relieve bone pain in this population of patients (31–33). Our observation in the current study that sRANK-Fc reduced several bone systemic bone parameters including OC, BAP, and Ntx in the mice with tumors is consistent with these results. We cannot determine from this study whether the alteration in bone remodeling markers was caused by direct effects of sRANK-Fc on bone or the diminished tumor growth and, thus, decreased tumor impact on bone, or even a combination of these events. Regardless, the presence of tumor was directly associated with increased bone remodeling, suggesting that the tumor has an

impact on bone physiology. This is consistent with our observation that CaP cells including LuCaP (current study), LNCaP, and C4–2B cells express a soluble form of RANKL (7), which can induce osteoclastogenesis.

A major impetus for exploring methods to inhibit RANKL other than OPG is the potential for OPG to act as a survival factor for tumor cells. Specifically, OPG blocked TRAIL-mediated apoptosis of myeloma cells (8) and CaP cells (9). Furthermore, proapoptotic factors such as TNF stimulate OPG secretion from CaP cell lines (34). Taken together, these findings suggest that OPG may function as a survival factor for CaP cells in the bone marrow for microenvironment. Recently, a Phase I clinical trial using either OPG or pamidronate, a bisphosphonate, in patients with either multiple myeloma or breast cancer with radiologically confirmed lytic bone lesions demonstrated comparable inhibition of osteoclast activity, based on NTx levels, between the two compounds (35). However, neither tumor response nor patient survival were evaluated in that study, thus the effect of administering OPG on cancer progression in the cancer patient is unknown at this time. Our observations that sRANK-Fc neither binds TRAIL (data not shown) nor blocks TRAIL-mediated apoptosis of CaP cells suggests that it may be a suitable mediator of RANKL inhibition for clinical use.

The observation that tumor progression was decreased by sRANK-Fc suggests several alternative mechanisms, including the possibility that sRANK-Fc mediates its inhibitory effects either directly on tumor cells or indirectly through its inhibitory effect on RANK and osteoclasts. Similarly, bisphosphonates reduce bone pain in men with CaP skeletal metastases; however, it is unknown whether this effect is caused by inhibiting osteoclastic activity or because of its ability to inhibit tumor cell growth (36–38). In the current study, sRANK-Fc neither inhibited tumor growth or viability *in vitro*, nor did it impact s.c. tumor growth *in vivo*. These observations, taken together with the finding that sRANK-Fc diminished tumor growth in bone, suggests that sRANK-Fc does not have a direct effect on tumor but rather mediates its tumor inhibitory effect indirectly through modulating bone remodeling. However, we cannot rule out that sRANK-Fc has direct inhibitory effect on CaP cells that is dependent on the bone microenvironment.

The observation that sRANK-Fc treatment reduced osteoclast numbers to control levels but only partially diminished indices of tumor-induced osteoblastic activity including BMD and histomorphometric parameters suggests that the tumor cells themselves have bone mineralizing ability that is independent of osteoclastic activity. Thus, because sRANK-Fc only partially reduced tumor volume, the remaining tumor may have promoted osteoblastic activity. This is an agreement with the finding that a CaP cell line injected into mouse bone produced osteoblastic lesions in the presence of low numbers of osteoclasts during the early stages of tumor growth (39). In addition to the pro-osteoblastic activity of tumor remaining after sRANK-Fc treatment, the reduction of osteoclast activity may have resulted in reduction of bone remodeling and, thus, inability of bone resorption to occur to restore the bone to control levels.

In summary, results from the current study demonstrate that an osteoblastic CaP xenograft, LuCaP, produces sRANKL-Fc and induces osteoclastogenesis *in vitro*. Furthermore, this study demonstrated that sRANK-Fc diminishes progression of established LuCaP in bone but not in s.c. tissue, which suggests that osteoblastic tumors require osteoclastic activity to progress and suggests that inhibiting RANKL in men with osteoblastic skeletal metastases will slow tumor progression. Finally, these data suggest that sRANK-Fc is an effective mediator of RANKL inhibition that does not block TRAIL-mediated apoptosis.

ACKNOWLEDGMENTS

We thank Dr. Robert Vessella for providing the LuCaP 35 xenograft.

REFERENCES

1. Abrams, H., Spiro, R., and Goldstein, N. Metastases in carcinoma. Cancer (Phila.), *3:* 74–85, 1950.
2. Charhon, S. A., Chapuy, M. C., Delvin, E. E., Valentin-Opran, A., Edouard, C. M., and Meunier, P. J. Histomorphometric analysis of sclerotic bone metastases from prostatic carcinoma special reference to osteomalacia. Cancer (Phila.), *51:* 918–924, 1983.
3. Urwin, G. H., Percival, R. C., Harris, S., Beneton, M. N., Williams, J. L., and Kanis, J. A. Generalised increase in bone resorption in carcinoma of the prostate. Br. J. Urol., *57:* 721–723, 1985.
4. Clarke, N. W., McClure, J., and George, N. J. Disodium pamidronate identifies differential osteoclastic bone resorption in metastatic prostate cancer. Br. J. Urol., *69:* 64–70, 1992.
5. Clarke, N. The effects of pamidronate disodium treatment in metastatic prostate cancer. Rev. Contemp. Pharamcother., *9:* 205–212, 1998.
6. Takahashi, N., Udagawa, N., and Suda, T. A new member of tumor necrosis factor ligand family, ODF/OPGL/TRANCE/RANKL, regulates osteoclast differentiation and function. Biochem. Biophys. Res. Commun., *256:* 449–455, 1999.
7. Zhang, J., Dai, J., Qi, Y., Lin, D. L., Smith, P., Strayhorn, C., Mizokami, A., Fu, Z., Westman, J., and Keller, E. T. Osteoprotegerin inhibits prostate cancer-induced osteoclastogenesis and prevents prostate tumor growth in the bone. J. Clin. Invest., *107:* 1235–1244, 2001.
8. Shipman, C. M., and Croucher, P. I. Osteoprotegerin is a soluble decoy receptor for tumor necrosis factor-related apoptosis-inducing ligand/Apo2 ligand and can function as a paracrine survival factor for human myeloma cells. Cancer Res., *63:* 912–916, 2003.
9. Holen, I., Croucher, P. I., Hamdy, F. C., and Eaton, C. L. Osteoprotegerin (OPG) is a survival factor for human prostate cancer cells. Cancer Res., *62:* 1619–1623, 2002.
10. Yano, Y., Hayashi, Y., Nakaji, M., Nagano, H., Seo, Y., Ninomiya, T., Yoon, S., Wada, A., Hirai, M., Kim, S. R., Yokozaki, H., and Kasuga, M. Different apoptotic regulation of TRAIL-caspase pathway in HBV- and HCV-related hepatocellular carcinoma. Int. J. Mol. Med., *11:* 499–504, 2003.
11. Smyth, M. J., Takeda, K., Hayakawa, Y., Peschon, J. J., van den Brink, M. R., and Yagita, H. Nature's TRAIL—on a path to cancer immunotherapy. Immunity, *18:* 1–6, 2003.
12. de Bono, J. S., and Rowinsky, E. K. Therapeutics targeting signal transduction for patients with colorectal carcinoma. Br. Med. Bull., *64:* 227–254, 2002.
13. Oyajobi, B. O., Anderson, D. M., Traianedes, K., Williams, P. J., Yoneda, T., and Mundy, G. R. Therapeutic efficacy of a soluble receptor activator of nuclear factor κB-IgG Fc fusion protein in suppressing bone resorption and hypercalcemia in a model of humoral hypercalcemia of malignancy. Cancer Res., *61:* 2572–2578, 2001.
14. Sordillo, E. M., and Pearse, R. N. RANK-Fc: a therapeutic antagonist for RANK-L in myeloma. Cancer (Phila.), *97:* 802–812, 2003.
15. Childs, L. M., Paschalis, E. P., Xing, L., Dougall, W. C., Anderson, D., Boskey, A. L., Puzas, J. E., Rosier, R. N., O'Keefe, R. J., Boyce, B. F., and Schwarz, E. M. In vivo RANK signaling blockade using the receptor activator of NF-κB:Fc effectively prevents and ameliorates wear debris-induced osteolysis via osteoclast depletion without inhibiting osteogenesis. J. Bone Miner. Res., *17:* 192–199, 2002.
16. Corey, E., Quinn, J. E., Buhler, K. R., Nelson, P. S., Macoska, J. A., True, L. D., and Vessella, R. L. LuCaP 35: a new model of prostate cancer progression to androgen independence. Prostate, *55:* 239–246, 2003.
17. Corey, E., Quinn, J. E., Bladou, F., Brown, L. G., Roudier, M. P., Brown, J. M., Buhler, K. R., and Vessella, R. L. Establishment and characterization of osseous prostate cancer models: intra-tibial injection of human prostate cancer cells. Prostate, *52:* 20–33, 2002.
18. Nemeth, J. A., Harb, J. F., Barroso, U., Jr., He, Z., Grignon, D. J., and Cher, M. L. Severe combined immunodeficient-hu model of human prostate cancer metastasis to human bone. Cancer Res., *59:* 1987–1993, 1999.
19. Pearse, R. N., Sordillo, E. M., Yaccoby, S., Wong, B. R., Liau, D. F., Colman, N., Michaeli, J., Epstein, J., and Choi, Y. Multiple myeloma disrupts the TRANCE/osteoprotegerin cytokine axis to trigger bone destruction and promote tumor progression. Proc. Natl. Acad. Sci. USA, *98:* 11581–11586, 2001.
20. Dai, J., Lin, D., Zhang, J., Habib, P., Smith, P., Murtha, J., Fu, Z., Yao, Z., Qi, Y., and Keller, E. T. Chronic alcohol ingestion induces osteoclastogenesis and bone loss through IL-6 in mice. J. Clin. Invest., *106:* 887–895, 2000.
21. Parfitt, A. M., Drezner, M. K., Glorieux, F. H., Kanis, J. A., Malluche, H., Meunier, P. J., Ott, S. M., and Recker, R. R. Bone histomorphometry: standardization of nomenclature, symbols, and units. Report of the ASBMR Histomorphometry Nomenclature Committee. J. Bone Miner. Res., *2:* 595–610, 1987.
22. Emery, J. G., McDonnell, P., Burke, M. B., Deen, K. C., Lyn, S., Silverman, C., Dul, E., Appelbaum, E. R., Eichman, C., DiPrinzio, R., Dodds, R. A., James, I. E., Rosenberg, M., Lee, J. C., and Young, P. R. Osteoprotegerin is a receptor for the cytotoxic ligand TRAIL. J. Biol. Chem., *273:* 14363–14367, 1998.
23. Berruti, A., Piovesan, A., Torta, M., Raucci, C. A., Gorzegno, G., Paccotti, P., Dogliotti, L., and Angeli, A. Biochemical evaluation of bone turnover in cancer patients with bone metastases: relationship with radiograph appearances and disease extension. Br. J. Cancer, *73:* 1581–1587, 1996.
24. Vinholes, J., Coleman, R., and Eastell, R. Effects of bone metastases on bone metabolism: implications for diagnosis, imaging and assessment of response to cancer treatment. Cancer Treat. Rev., *22:* 289–331, 1996.

25. Roudier, M., Sherrard, D., True, L., Ott-Ralp, S., Meligro, C., MBerrie, M., Soo, C., Felise, D., Quinn, J. E., and Vessella, R. Heterogenous bone histomorphometric patterns in metastatic prostate cancer. J. Bone Miner. Res., *15S1:* S567, 2000.
26. Yonou, H., Kanomata, N., Goya, M., Kamijo, T., Yokose, T., Hasebe, T., Nagai, K., Hatano, T., Ogawa, Y., and Ochiai, A. Osteoprotegerin/osteoclastogenesis inhibitory factor decreases human prostate cancer burden in human adult bone implanted into nonobese diabetic/severe combined immunodeficient mice. Cancer Res., *63:* 2096–2102, 2003.
27. Guise, T. A. Molecular mechanisms of osteolytic bone metastases. Cancer (Phila.), *88:* 2892–2898, 2000.
28. Clarke, N. W., McClure, J., and George, N. J. Morphometric evidence for bone resorption and replacement in prostate cancer. Br. J. Urol., *68:* 74–80, 1991.
29. Garnero, P., Buchs, N., Zekri, J., Rizzoli, R., Coleman, R. E., and Delmas, P. D. Markers of bone turnover for the management of patients with bone metastases from prostate cancer. Br. J. Cancer, *82:* 858–864, 2000.
30. Fontana, A., and Delmas, P. D. Markers of bone turnover in bone metastases. Cancer (Phila.), *88:* 2952–2960, 2000.
31. Dawson, N. A. Therapeutic benefit of bisphosphonates in the management of prostate cancer-related bone disease. Expert Opin. Pharmacother., *4:* 705–716, 2003.
32. Pelger, R. C., Hamdy, N. A., Zwinderman, A. H., Lycklama a Nijeholt, A. A., and Papapoulos, S. E. Effects of the bisphosphonate olpadronate in patients with carcinoma of the prostate metastatic to the skeleton. Bone, *22:* 403–408, 1998.
33. Heidenreich, A., Hofmann, R., and Engelmann, U. H. The use of bisphosphonate for the palliative treatment of painful bone metastasis due to hormone refractory prostate cancer [In Process Citation]. J. Urol., *165:* 136–140, 2001.
34. Penno, H., Silfversward, C. J., Frost, A., Brandstrom, H., Nilsson, O., and Ljunggren, O. Osteoprotegerin secretion from prostate cancer is stimulated by cytokines, in vitro. Biochem. Biophys. Res. Commun., *293:* 451–455, 2002.
35. Body, J. J., Greipp, P., Coleman, R. E., Facon, T., Geurs, F., Fermand, J. P., Harousseau, J. L., Lipton, A., Mariette, X., Williams, C. D., Nakanishi, A., Holloway, D., Martin, S. W., Dunstan, C. R., and Bekker, P. J. A phase I study of AMGN-0007, a recombinant osteoprotegerin construct, in patients with multiple myeloma or breast carcinoma related bone metastases. Cancer (Phila.), *97:* 887–892, 2003.
36. Corey, E., Brown, L. G., Quinn, J. E., Poot, M., Roudier, M. P., Higano, C. S., and Vessella, R. L. Zoledronic acid exhibits inhibitory effects on osteoblastic and osteolytic metastases of prostate cancer. Clin. Cancer Res., *9:* 295–306, 2003.
37. Coleman, R. E. Optimising treatment of bone metastases by Aredia™ and Zometa™. Breast Cancer, *7:* 361–369, 2000.
38. Boissier, S., Ferreras, M., Peyruchaud, O., Magnetto, S., Ebetino, F. H., Colombel, M., Delmas, P., Delaisse, J. M., and Clezardin, P. Bisphosphonates inhibit breast and prostate carcinoma cell invasion, an early event in the formation of bone metastases. Cancer Res., *60:* 2949–2954, 2000.
39. Lee, Y., Schwarz, E., Davies, M., Jo, M., Gates, J., Wu, J., Zhang, X., and Lieberman, J. R. Differences in the cytokine profiles associated with prostate cancer cell induced osteoblastic and osteolytic lesions in bone. J. Orthop. Res., *21:* 62–72, 2003.